frontiers | Frontiers in Energy Research

TYPE Original Research
PUBLISHED 15 November 2023
DOI 10.3389/fenrg.2023.1297866

OPEN ACCESS

EDITED BY
Tingting Zhu,
University of Twente, Netherlands

REVIEWED BY
Yingying Yang,
University of Shanghai for Science and Technology, China
Ye Liu,
Xi'an Jiaotong University, China

*CORRESPONDENCE
Libiao Zhang,
lbzhang4@163.com

RECEIVED 20 September 2023
ACCEPTED 24 October 2023
PUBLISHED 15 November 2023

CITATION
Zhang L, Jing W, Wang Q, Zhang J and Yang P (2023), Energy and emission performance of enhanced vapor injection air source heat pump system using low global warming potential refrigerants in different climate regions.
Front. Energy Res. 11:1297866.
doi: 10.3389/fenrg.2023.1297866

Energy and emission performance of enhanced vapor injection air source heat pump system using low global warming potential refrigerants in different climate regions

Libiao Zhang[1]*, Wuhui Jing[1], Qilong Wang[2], Jianing Zhang[2] and Peifang Yang[2]

[1]Zhejiang King Co., Ltd., Shangyu, China, [2]Tianjin Key Laboratory of Refrigeration Technology, Tianjin University of Commerce, Tianjin, China

In order to meet the space heating requirement of residential buildings in low-temperature areas, the performance of the enhanced vapor injection (EVI) air source heat pump (ASHP) system and single-stage compression heat pump system (BASE) using low global warming potential (GWP) working fluids in low-temperature environment are studied. The thermodynamic and emission characteristic models of air source heat pump are developed and optimized, and further compared with traditional heating solutions when used in five different typical cities throughout the world. The results indicate among the selected working fluids, R152a achieves the highest COP of 3.91 among all of the selected low GWP working fluids. When the ambient temperature is 0°C, the maximum COP of the EVI system is 2.51 when CO_2 is adopted, and the corresponding optimal discharge pressure and intermediate pressure are 10.57 MPa and 3.83 MPa, respectively. By exploring the changes of HSPF in five typical cities, the HSPF of the EVI system using CO_2 is the most significant, which is 17.13%–26.69% higher than the BASE system. The most significant reduction of LCCP in EVI system using CO_2 is 15.34%–26.66% compared with BASE system. For SO_2 and NO_X, the EVI system using R152a has a better emission reduction effect, which is 3.73%–64.73% and 3.72%–66.04% lower than the other solutions, respectively. This study can provide a theoretical reference for the application of low GWP heat pumps with EVI technology.

KEYWORDS

enhanced vapor injection, air source heat pump, low global warming potential, heating seasonal performance factor, carbon and pollutant emissions

1 Introduction

1.1 Background

With the exacerbation of energy crisis and environmental contamination, the heating technology needs to be constantly innovated (Farghali et al., 2023). Air source heat pump (ASHP) is considered as an environmental space heating method with the advantage of safety and reliability, which is widely used in rural areas of North China. ASHP is chosen as a key solution to replace traditional fossil fuel boilers (Mateu-Royo et al., 2021; IEA, 2023).

Most air source heat pump uses traditional synthetic refrigerants, including R410A, R134a, R22, etc. These hydrofluorocarbons (HFCs) and hydrochlorofluorocarbons (HCFCs) with high global warming potential (GWP) can cause serious greenhouse effects. The Montreal Protocol stipulates that developing countries must completely prohibit the use of HCFCs by 2040. Therefore, the development of green refrigerants with low GWP must be taken seriously, which includes natural refrigerants [CO_2, hydrocarbons (HCs), etc.], and synthetic working fluids [R161, R152a, hydrofluoroolefins (HFOs), etc.]. Among them, CO_2 operates in the transcritical mode (Wu et al., 2021), while others are in the subcritical mode when heating. CO_2 is regarded as a refrigerant with broad application prospects because of its environmental protection, non-toxic and non-flammable characteristics (Lorentzen, 1994).

However, when the heat pump works in the regions with relatively low ambient temperature, the compression ratio is relatively high, leading to the reduction of the compressor efficiency, increasing of compressor discharge temperature as well as the degradation in the energy efficiency of the ASHP. In order to solve the problem of system performance deterioration, the technique of enhanced vapor injection (EVI) is applied to solve the problem of high compression ratio and widen the application of ASHP in low-temperature regions.

1.2 Literature review

Many studies about the performance of ASHP with EVI were conducted and reported, including the selection of working fluids, system configurations, and characteristics of changing operating conditions.

In terms of refrigerant selection (Guo et al., 2023), conducted an experimental study on the heating performance of the ASHP integrated with a flash tank using R410A in cold areas and found that the heating capacity increases by 3.84 kW compared with the basic system (Xu et al., 2013). Studied the performance difference of ASHP with EVI using R410A and R32, which indicates that the system using R32 can increase capacity and COP by 10% and 9%, respectively (de Carvalho et al., 2019). Evaluated five different binary hydrocarbon mixtures used in the heat pump system with EVI and concluded that the performance increases by 4%–36%. Moreover, the EVI heat pump system adopting low GWP as the refrigerant has also been widely concerned (Maeng et al., 2023). Compared the performance of EVI heat pump system with a flash tank by employing three working fluids (R152a, R1234yf, and R134a). The results show that R152a is recommended as the preferred alternative due to its high COP and low emissions.

Moreover, many scholars have made efforts in system configuration optimization (Zhang et al., 2016). Established an ASHP with vapor injection using economizer test facility in cold regions of China, which showed that the thermal performance of EVI-ASHP is improved by 4%–6% (Yang et al., 2022). Introduced a heat pump system with flash tank. The heating performance of the system was experimentally studied. By comparing with the single-stage compression system, it can be seen that the heating effect after using EVI technology, and the lower the ambient temperature, the better the progress (Heo et al., 2010). Studied the effect of a compressor with EVI on the performance of the system and found that the COP and heating capacity enhanced by 10% and 25% (Zhao and Yu, 2023). Proposed an improved subcooler vapor-injection (MSV) cycle with an ejector for ASHP utilizations, and the results show that this system has better heating performance. Li et al. (2023) studied the effects of upstream injection path and downstream injection path configurations on the flash tank vapor injection and economizer vapor injection. In contrast, flash tanks have an advantage in heating at −15°C (Dai et al., 2022). Studied air source heat pumps and developed four hybrid configurations combined with EVI and mechanical subcooling technology.

In order to achieve the purpose of energy conservation and pollutant reduction, low GWP CO_2 is applied to the ASHP with EVI and studied in detail. Many scholars have studied the vapor injection transcritical CO_2 heat pump system with the flash tank (VI-ET). For the study of variable working conditions (Chung et al., 2018), studied the VI-ET in extremely cold and hot environments. The results show that comparison with the base system, the heating efficiency of the CO_2 heat pump system with EVI increases by 7.1% (Peng et al., 2020). Studied the utilization of CO_2 heat pump systems with EVI in the domain of power vehicles at the ambient temperatures of 0°C and 5°C and found the COP ranged from 2.0 to 2.4. The results showed that CO_2 heat pump systems with EVI were more adequacy for electric vehicles working in cold regions (Sun et al., 2023). Optimized the structure of the

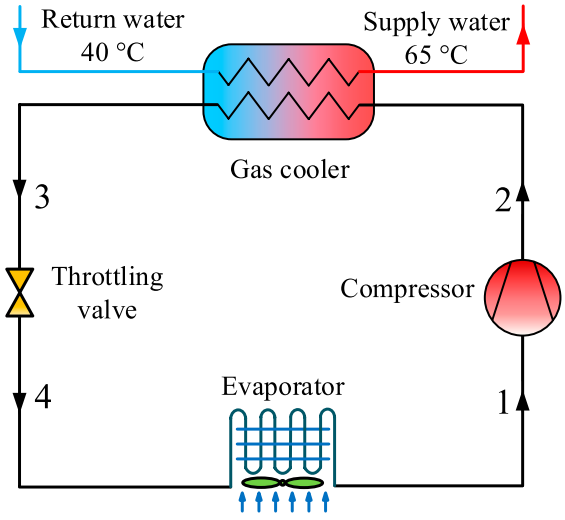

FIGURE 1
The diagram of BASE system.

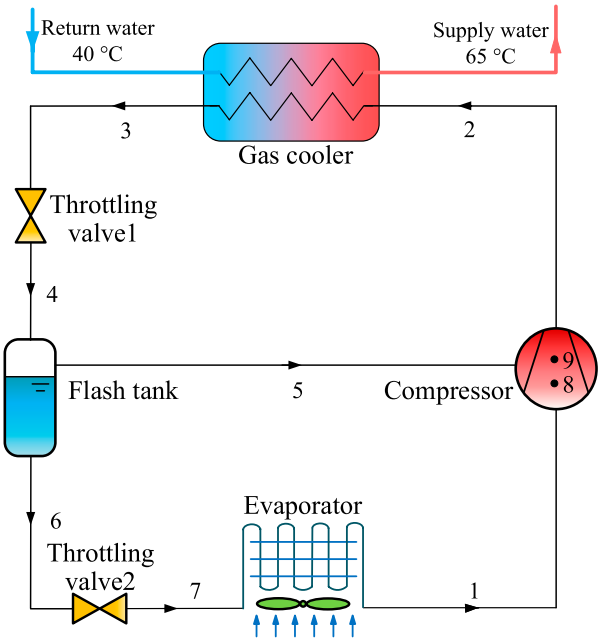

FIGURE 2
The diagram of EVI system.

VI-ET system, which effectively controlled the two-phase injection in the flash tank.

Moreover, many researchers have studied the configuration and optimization of models for vapor-injection heat pump systems (Qiao et al., 2015). Explored the dynamic behavior of VI-ET from the perspective of numerical modeling and established a first-principles transient model (Yang et al., 2023). Established a transcritical CO_2 heat pump system for the VI-ET of electric vehicles and proposed a control strategy based on COP adjustment sequence and judgment basis (Liu et al., 2023). Conducted an experimental investigation on the performance of a transcritical CO_2 heat pump using a VI-ET system. The results show that comparison with a revolution ratio of 1, changing the revolution ratio can increase COP by 7% and reduce discharge pressure by 0.85 MPa. When the revolution ratio is less than 1 and the near revolution ratio is about 0.89, COP reaches a peak of 1.98. For the configuration of the flash tank (Wang and Li, 2019), used the extremum method to optimize the intermediate pressure of the VI-ET system. Based on the dynamic simulation model of modelica simulation software, the effectiveness of the control strategy is verified.

1.3 Scope and contribution

Based on the above documents, we can see that the technology of enhanced vapor injection is an available solution to improve COP, especially in cold regions. However, most of the previous work only focuses on the system performance using only one or several refrigerants, while the working fluid used for the EVI heat pump system has a critical impact on the thermodynamic and emission performance. Furthermore, the carbon emissions and the pollutant emissions when EVI heat pump is utilized for space heating are also seldom evaluated, when used in different climate regions.

To estimate the working fluid selection on the system performance, low GWP working fluids are selected as the promising candidates, and a comparison of energy efficiency and emission performance between the basic ASHP system and the ASHP system with EVI is conducted. Additionally, the carbon and pollutant emissions reduction potential when EVI technology is adopted for ASHP is also assessed, which can provide a reference for the working selection and emission reduction evaluation for the ASHP system used in different climate regions.

2 System description

2.1 Basic heat pump system

The schematic diagram of the basic heat pump system (BASE) is shown in Figure 1. When the ambient temperature is low, the evaporation temperature of the system is low and the compression ratio is high, which leads to a higher discharge temperature and a lower efficiency of the compressor. As a result, the system performance is poor. In order to ensure that the BASE system still has high heating performance at low temperatures, the vapor injection technology combined with the flash tank is introduced to reduce the discharge pressure.

2.2 Heat pump system with EVI

The CO_2 vapor injection heat pump system (EVI) with the flash tank shown in Figure 2, which consists of a quasi-two-stage compressor, a gas cooler, two throttle valves, a flash tank, and an evaporator. As a key component, the flash tank can separate the gas-phase and liquid-phase refrigerants, which can help to reduce the enthalpy at the evaporator inlet (Xu et al., 2011). In this system, the refrigerant at the outlet of the gas cooler enters the flash tank in a gas-liquid two-phase state after throttling. Due to the decrease in the flowing speed of the working fluid, the vapor and liquid are separated. The vapor is mixed with the superheated gas of state 8 for recompression to state 9 indicated in the figure. The liquid separated from the flash tank enters the evaporator to absorb heat from the ambient air after secondary throttling. The standard working condition is set as ambient temperature of 0°C, and the temperature of supply and return water is 65°C and 40°C, respectively.

Figure 3 is the temperature entropy diagram of BASE system and EVI system using CO_2 and R410A, respectively. For natural working fluid CO_2, it operates in a transcritical cycle mode, due to its relatively low critical temperature of 31.1°C. In contrast, for R410A, which is selected as a representative of traditional synthetic working fluid, it runs in subcritical cycle mode because of the high critical temperature. In the Figures 3B, D, it can be found that the specific enthalpy of the evaporator inlet is reduced by employing EVI compared with that shown in Figures 3A, C, which can effectively improve the heat absorption capacity of the evaporator, thereby improving the heating energy efficiency of the ASHP system for space heating.

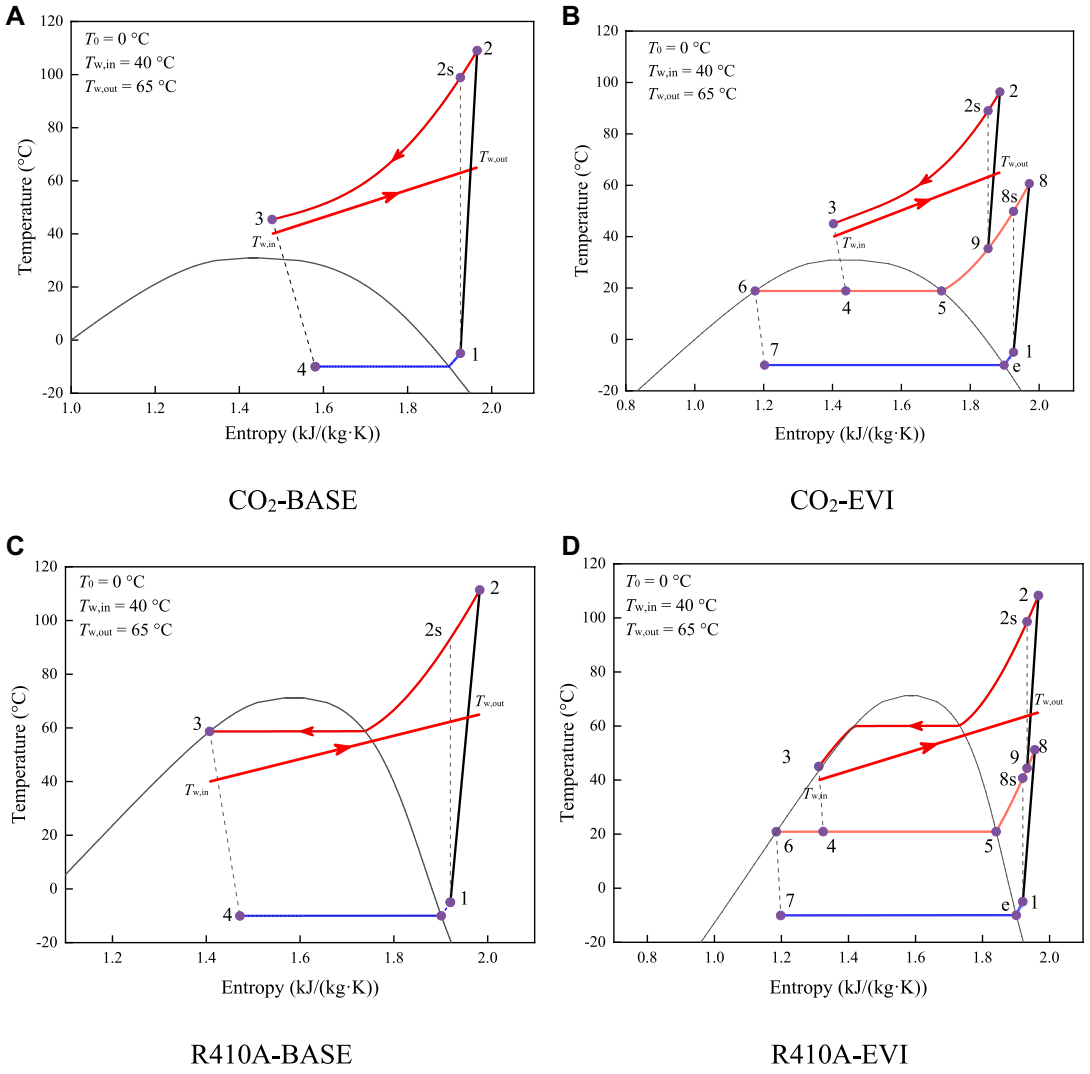

FIGURE 3
T-s diagram of BASE and EVI for CO_2 and traditional synthetic refrigerant. **(A)** CO_2-BASE. **(B)** CO_2-EVI. **(C)** R410A-BASE. **(D)** R410A-EVI.

TABLE 1 The properties of refrigerants.

Substance	Physical data				Environmental data		
	Molecular mass	T_b (°C)	T_c (°C)	p_c (MPa)	Atmospheric life (year)	ODP	GWP
R744	44.01	−78.4	31.1	7.38	>50	0	1
R410A	72.58	−51.4	71.4	4.9	—	0	2,100
R32	52.02	−51.7	78.1	5.78	4.9	0	675
R152a	66.05	−24.0	113.3	4.52	1.4	0	124
R1234yf	114.04	−29.5	94.7	3.38	0.029	0	<4.4
R161	48.06	−37.6	102.2	5.09	0.21	0	12
R134a	102.03	−26.1	101.1	4.06	14	0	1,370
R1234ze (E)	114.04	9.0	153.6	3.97	0.045	0	<6

TABLE 2 Typical cities heating design parameters (ANSI/ASHRAE, 2013).

Parameter	Typical cities				
	Washington	Stockholm	Moscow	Harbin	Ulaanbaatar
Outdoor design heating temperature (°C)	−6.3	−9.9	−18.6	−25.2	−34.0
design heating load (W/m^2)	75.20	77.06	70.70	75.79	78.32
heating area (m^2)	200				

3 Methodology

3.1 Assumption of the model

The thermodynamic model is proposed based on the below hypothesis:

(1) The system works under a steady running state (Peng et al., 2020);
(2) The heat loss of the system components is 4% (Llopis et al., 2016);
(3) The heat loss of the equipment and pressure drop of the fluid flowing through the pipelines are ignored (Wang et al., 2019);
(4) The ambient temperature is 10°C higher than the evaporation temperature (He et al., 2021).

3.2 Energetic model

3.2.1 Baseline transcritical CO_2 combined heat pump system

For the system researched, the energy performance can be obtained (Gullo et al., 2016).

$$W_{\mathrm{Comp,BASE}} = m_{\mathrm{CO_2}}(h_2 - h_1) \tag{1}$$

$$\eta_{\mathrm{g,CO_2}} = -0.0021(p_{\mathrm{h}}/p_{\mathrm{l}})^2 - 0.0155(p_{\mathrm{h}}/p_{\mathrm{l}}) + 0.7325 \tag{2}$$

where p_{l} and p_{h} represent the suction and discharge pressure of the compressor.

The heat capacity and COP are shown as follows:

$$Q_{\mathrm{H,BASE}} = m_{\mathrm{CO_2}} \cdot (h_2 - h_3) \tag{3}$$

$$\mathrm{COP_{BASE}} = \frac{Q_{\mathrm{H,BASE}}}{W_{\mathrm{Comp,BASE}}} \tag{4}$$

3.2.2 CO_2 heat pump system with enhanced vapor injection

The power consumption and efficiency of the vapor injection compressor can be expressed as:

$$W_{\mathrm{Comp,EVI}} = m_{\mathrm{CO_2}}(h_2 - h_9) + m_6(h_8 - h_1) \tag{5}$$

$$\eta_{\mathrm{g,l,CO_2}} = -0.0012(p_{\mathrm{m}}/p_{\mathrm{l}})^2 - 0.0087(p_{\mathrm{m}}/p_{\mathrm{l}}) + 0.6692 \tag{6}$$

$$\eta_{\mathrm{g,h,CO_2}} = -0.0021(p_{\mathrm{h}}/p_{\mathrm{m}})^2 - 0.0155(p_{\mathrm{h}}/p_{\mathrm{m}}) + 0.7325 \tag{7}$$

where, p_{m} is the intermediate pressure; $\eta_{\mathrm{g,l,CO2}}$ and $\eta_{\mathrm{g,h,CO2}}$ are the global efficiency of CO_2 subcritical and transcritial compressor, respectively.

The COP and the heating capacity per unit volume can be obtained:

$$Q_{\mathrm{H,EVI}} = m_{\mathrm{CO_2}}(h_2 - h_3) \tag{8}$$

$$q_{\mathrm{v}} = Q_{\mathrm{H,EVI}} \cdot \rho \tag{9}$$

$$\mathrm{COP_{EVI}} = \frac{Q_{\mathrm{H,EVI}}}{W_{\mathrm{Comp,EVI}}} \tag{10}$$

3.3 Emission performance model

Considering the direct and indirect CO_2 emissions of the heat pump system, LCCP is used to evaluate the equivalent CO_2 emissions of a heat pump system throughout its life cycle (Lee et al., 2016).

$$\mathrm{LCCP} = \mathrm{LCCP_{direct}} + \mathrm{LCCP_{indirect}} \tag{11}$$

SO_2, NO_X, $PM_{2.5}$, and PM_{10} are selected as key factors to evaluate the energy-saving and emission reduction effect of EVI systems within the life cycle. The formulas for calculating pollutant emissions are expressed as follows (Dai et al., 2020).

For electric heating boilers and EVI systems:

$$m_{\mathrm{emis}} = E \cdot \mu_{\mathrm{emis}} \tag{12}$$

For coal-fired boilers and gas-fired boilers:

$$m_{\mathrm{emis}} = M \cdot \mu_{\mathrm{emis}} \tag{13}$$

3.4 Working fluid selection

The selection of refrigerant is very important to the performance and emission characteristics of heat pumps. Eight kinds of working fluid are selected to be used in ASHP, including 6 low GWP working fluids and 2 widely used HFCs (R410A and R134a), and the latter two HFCs with relatively high GWP are used for comparison. The properties of the candidate working fluids are shown in Table 1.

3.5 Seasonal performance model

Five typical cities in different climate regions, including Washington, Stockholm, Moscow, Harbin, and Ulaanbaatar, are selected to evaluate the carbon emission and pollutant emission effects of the EVI system. The heating design parameters of four typical cities are shown in Table 2.

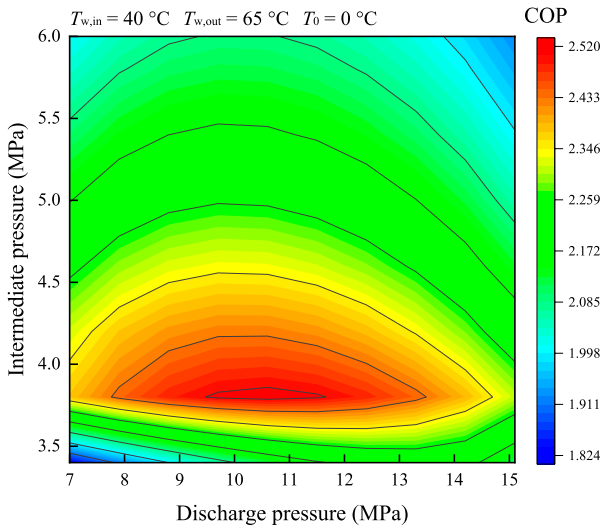

FIGURE 4
Variation of COP with discharge pressure and intermediate pressure.

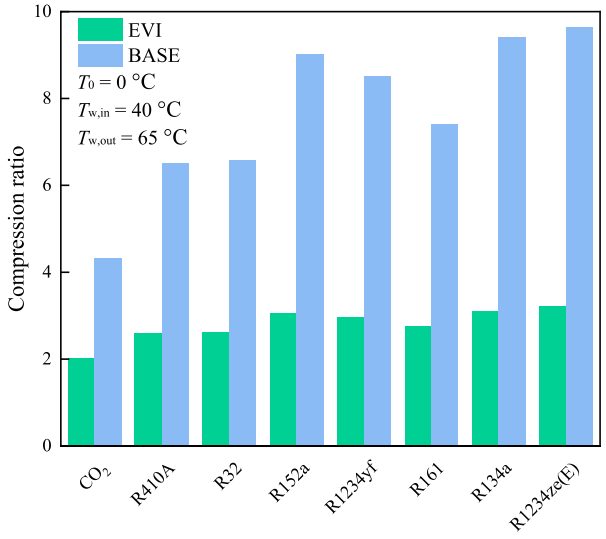

FIGURE 6
The change of compression ratio of system with different refrigerants.

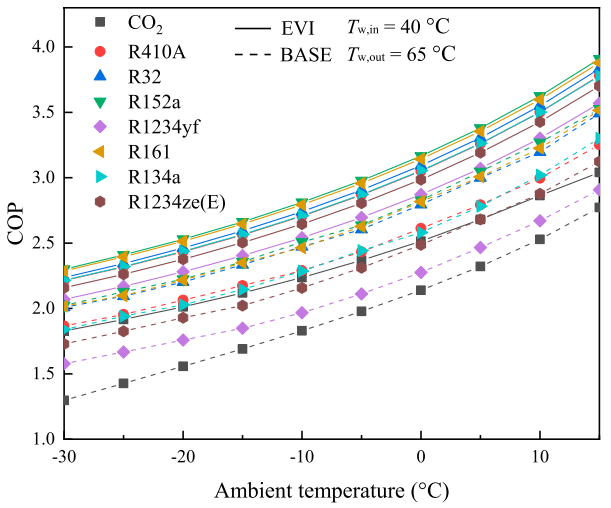

FIGURE 5
COP varying with ambient temperature.

Based on the design heat load ($q_{H,desi}$), outdoor design heating temperature ($T_{H,desi}$) and ambient hourly temperature ($T_{0,h}$), the hourly heat load [$q_H(i)$] of the house can be determined (Dai et al., 2022):

$$\dot{q}_H(i) = \dot{q}_{H,desi}\left(\frac{T_h - T_{0,h}}{T_h - T_{h,desi}}\right) \tag{14}$$

The heating capacity in the heating season is:

$$\dot{Q}_H = \sum_{i=1}^{n} \dot{q}_H(i) \cdot A \tag{15}$$

The hourly power consumption of the system is expressed as:

$$\dot{W}_H(i) = \frac{\dot{q}_H(i) \cdot A}{COP} \tag{16}$$

where A is the heating area of the house, set to 200 m^2.

Therefore, the heating seasonal performance factor (HSPF) of the CO_2 heat pump system is expressed as follows (Ghoubali et al., 2014):

$$HSPF = \frac{\dot{Q}_H}{\dot{W}_H} \tag{17}$$

4 Results

4.1 Thermal-mechanical performance

Figure 4 shows the variation of COP with discharge pressure (p_h) and intermediate pressure (p_m) under standard operating conditions when CO_2 is used in the EVI system. It can be noted that with the increase of p_h and p_m, COP increases first and then decreases, and there is a maximum COP. The COP_{max} is 2.51, and the corresponding optimal p_h and p_m are 10.57 MPa and 3.83 MPa, respectively. The optimal p_h value can be explained by the S-shaped isotherm in the p-h plot (Dai et al., 2018). The discharge pressure and intermediate pressure have a notable effect on the overall performance of the system. The following analysis of the CO_2 system is based on the optimum operating condition of each system.

The variation of COP with environment temperature is shown in Figure 5. It can be seen that with the environment temperature enhances, COP gradually increases. The overall COP of the EVI system is higher than that of the BASE system. Among the 8 working fluids selected, the EVI system with R152a has the highest COP of 3.91 at the ambient temperature of 15°C, and the EVI system with CO_2 has the lowest COP of 3.04. For the same working fluid, the COP is significantly higher than

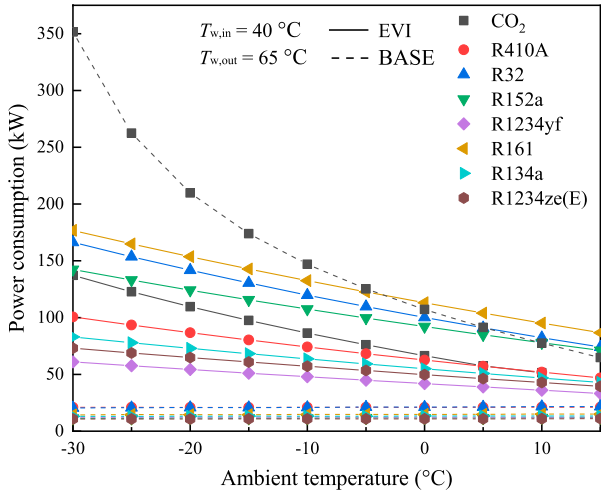

FIGURE 7
Power consumption varying with ambient temperature.

that of the BASE system. As far as CO_2 is concerned, the increase rate of COP is as high as 9.66%–40.85% at the ambient temperature range of −30°C–15°C. And the lower the ambient temperature, the higher the COP increase rate. It is proved that the EVI system is more practical for low ambient temperature.

Figure 6 describes the change in the compressor pressure ratio of the system with different working fluids under standard working conditions. For different working fluids, the overall compression ratio of the EVI system is obviously lower than that of the BASE system. The compression ratio of R1234ze (E) is the highest, which is 10.03 in the BASE system and 3.22 in the EVI system. The compression ratio of CO_2 is the lowest, which is 4.31 in the BASE system and 2.03 in the EVI system. The compression ratio of the EVI system with the CO_2 working medium is 52.9% lower than that of the BASE system. The compression ratio of the system is low and the exhaust pressure is reduced, which can prolong the service life of the compressor and enhance the overall energy efficiency of the cycle.

The power consumption of two systems with different working fluids varies with the environmental temperature as illustrated in Figure 7. Except for CO_2, the power consumption of EVI system is significantly higher than that of BASE system. And the lower the ambient temperature, the more obvious the power consumption of the EVI system. Among them, the increase of R161 is the most obvious. When the environmental temperature is −30°C, the power consumption of the EVI system with R161 is 176.80 kW, while the power consumption of the BASE system is 14.36 kW. The power consumption increased by 11.31 times. CO_2 working fluid shows the opposite trend and the power consumption of the BASE system with CO_2 is higher than that of the EVI system. Under the same severe working condition of −30°C, the power consumption of the EVI system with CO_2 is 137.78 kW, which is 60.98% lower than that of the BASE system. Combined with a lower compression ratio, the enhanced vapor injection compressor is more suitable for low-temperature environments than a single-stage compressor.

The heating capacity per unit volume of the 8 working fluids in BASE and EVI varies with the environmental temperature as described in Figure 8. The EVI system with R161 has the maximum heating capacity per unit volume, while the EVI system with CO_2 has the minimum. With the change in ambient temperature, the heating capacity per unit volume of CO_2 does not change much. Compared with the EVI system, the heating capacity per unit volume of the BASE system is slightly higher by 2.59%–15.15%. However, the changing trend of the other refrigerants is the opposite. The unit volume heating capacity of the EVI system is much higher than that of the BASE system at the same ambient temperature. Among them, the difference of R152a is the most obvious, and the heating capacity per unit volume of EVI system is 81.10%–232.80% higher than BASE system. In the

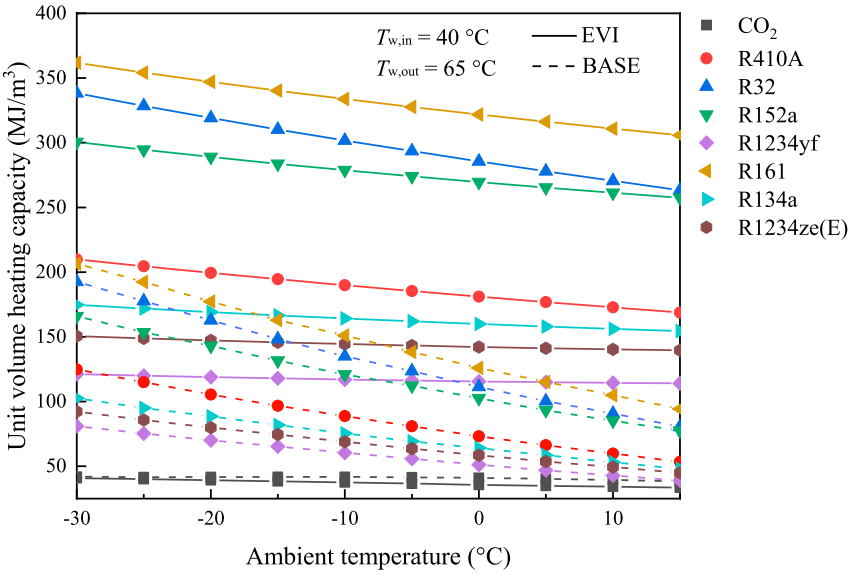

FIGURE 8
Variation of the unit volume heating capacity with environmental temperature.

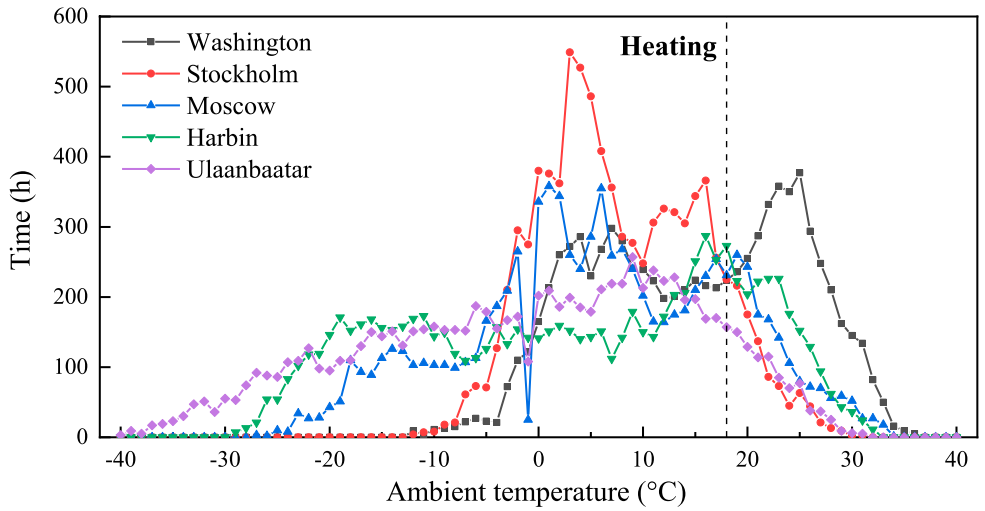

FIGURE 9
Temperature data distribution of the five representative cities.

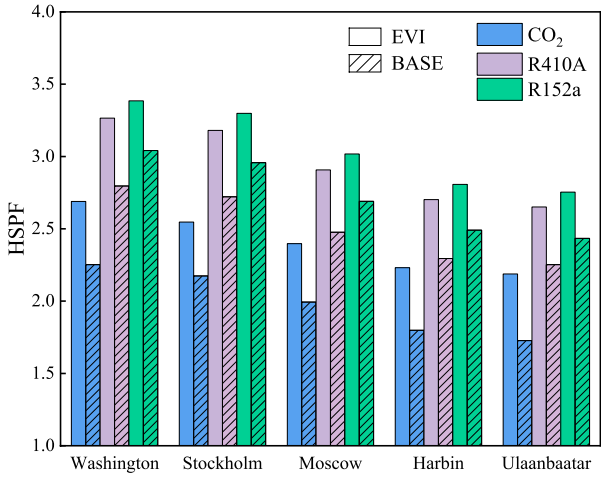

FIGURE 10
HSPF of the two ASHP systems in the five typical cities.

same system, CO_2 has the lowest unit volume heating capacity and relatively high power consumption, which results in a lower COP.

4.2 Heating seasonal performance coefficient

According to the weather data collected by the special meteorological data for building thermal environment analysis, the distribution of environmental temperature in the five typical cities is shown in Figure 9. Among them, Washington, Stockholm, Moscow, Harbin, and Ulaanbaatar represent the typical climate of five regions: mixed region, cool region, cold region, severe cold region and polar region. When the environmentalt temperature is lower than 18°C, space heating is needed. In order to evaluate the seasonal characteristics of the EVI system, the heating seasonal performance factor (HSPF) is selected as the comprehensive energy efficiency index to evaluate the heating performance.

The heating season performance coefficients by using different low GWP working fluids of the five typical cities are studied. According to the results indicated in Figure 5, the COP of R152a performs the highest COP during all the selected refrigerants. Consequently, R152a is chosen as the representative of low GWP working fluid operating with the subcritical cycle. Then, CO_2 works with the transcritical cycle and is also further studied. Moreover, the traditional synthetic working fluid R410A is also selected to compare with the two typical working fluids of R152a and CO_2, and the results are shown in Figure 10. It can be noted with the reduction of environmental temperature, the HSPF of each city showed a downward trend. The EVI system using R152a shows the best performance, while the EVI system using CO_2 shows the worst performance. When the EVI system uses R152a and CO_2, it has the highest and lowest HSPF, which are 3.38 and 1.73, respectively. In contrast with the BASE system, the HSPF of the EVI system isobviously improved. In the five cities, the EVI system using CO_2, R410A, and R152a is 17.13%–26.69%, 11.29%–13.15%, and 16.75%–17.74% higher than BASE system, respectively. Additionally, the lower the annual average temperature, the more obvious the system performance improvement. Compared with the other two working fluids, the EVI system with CO_2 has the most obvious performance improvement in low-temperature areas, among which Harbin and Ulaanbaatar have increased by 24.02% and 26.69%, respectively. Therefore, the EVI system is more suitable for low ambient temperature areas than high-temperature areas.

4.3 Analysis of emission characteristics

In order to evaluate the carbon emissions of different systems applied in residential buildings, the life cycle climate performance (LCCP) of five typical cities is evaluated, and the results are displayed in Figure 11. Among the six selected solutions, the LCCP of the EVI

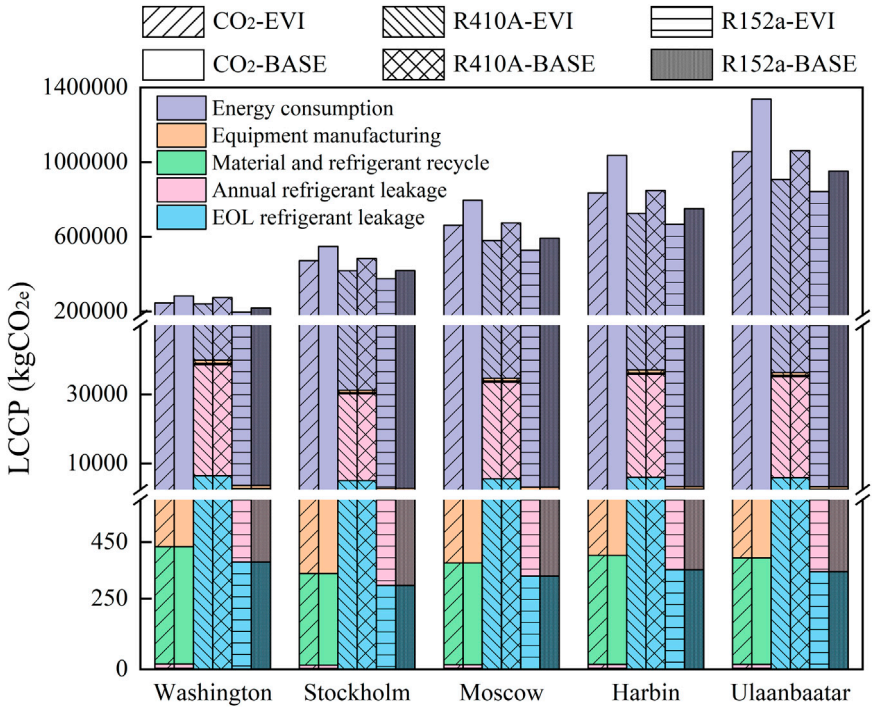

FIGURE 11
LCCP of the two ASHP systems in the five typical cities.

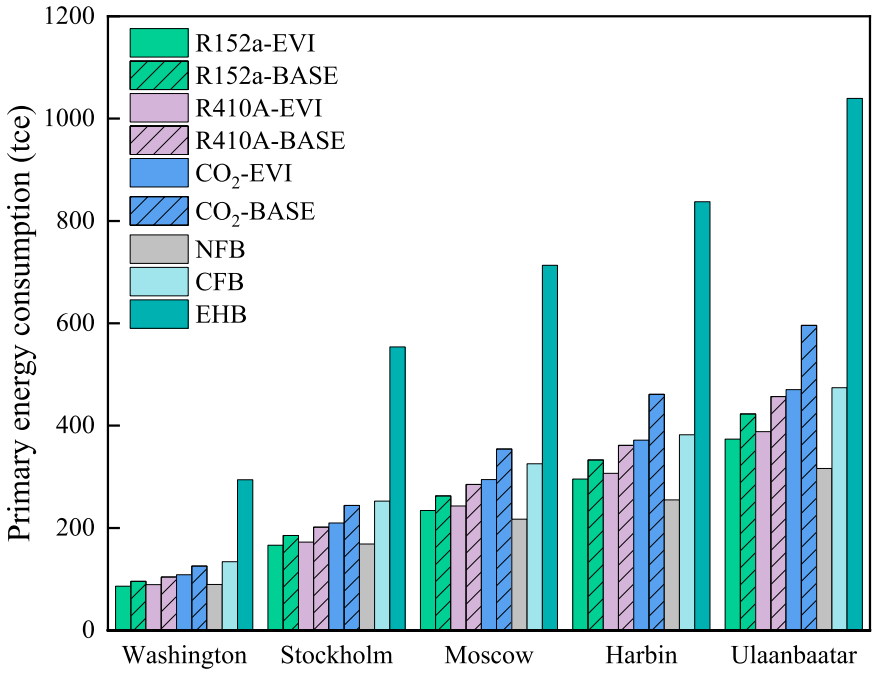

FIGURE 12
Primary energy consumption of typical cities.

system is generally smaller than that of the BASE system, and the system using R152a refrigerant has the least carbon emissions, while the system using CO_2 is the opposite. Taking Harbin as an example, the highest and lowest LCCP are the BASE system using CO_2 and the EVI system using R152a, respectively, which are 1035921.178 kg CO_{2e} and 666525.2706 kg CO_{2e}, respectively. It can be seen that carbon emissions from energy consumption dominate the LCCP, and the lower the ambient temperature of the city, the higher the proportion

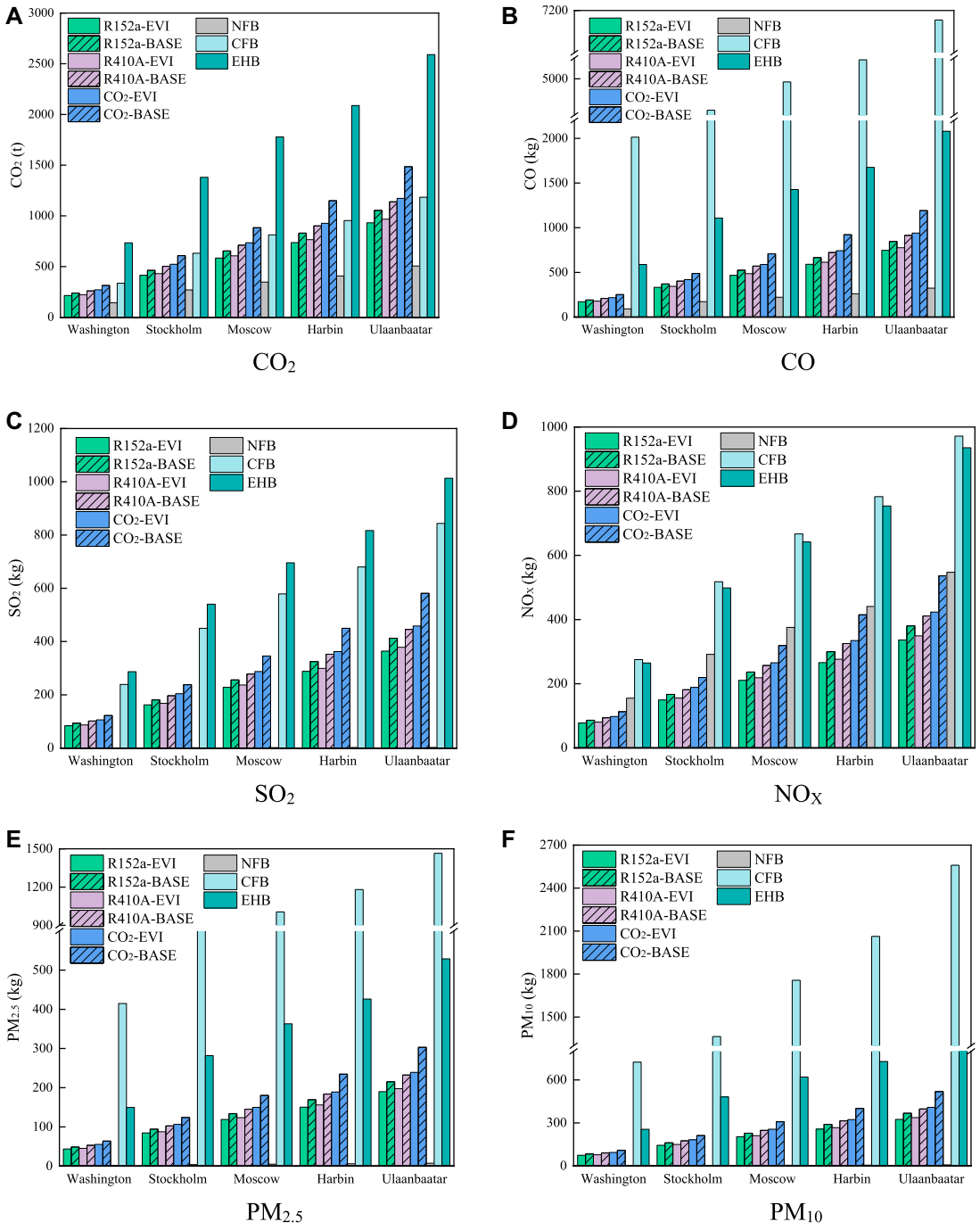

FIGURE 13
Life cycle pollutant emissions of different heating solutions. **(A)** CO_2. **(B)** CO. **(C)** SO_2. **(D)** NO_X. **(E)** $PM_{2.5}$. **(F)** PM_{10}.

of CO_2 emissions caused by energy consumption. Among the six solutions, energy consumption carbon emissions account for 83.38%–99.90% of total carbon emissions. The EVI system performs better than the BASE system in terms of carbon emission reduction. Compared with the BASE system using the same working fluid, the LCCP of the EVI system using CO_2, R410A, and R152a decreased by 15.34%–26.66%, 13.97%–17.01%, and 11.09%–13.10%, respectively. Compared with the BASE system, the EVI system can reduce carbon emissions by 12.53%–20.85% which is caused by energy consumption. The lower the ambient temperature, the higher the emission reduction rate, which further proves that the EVI system has a great advantage in low-temperature environment.

Figure 12 shows the primary energy consumption (PEC) of five typical cities in different climate regions. The change of ambient temperature and the consumption of primary energy show the opposite trend. The PEC of heating by electric heating boilers (EHB) is the highest, which is 294.27 tce ~1,038.35 tce. The best energy saving solution is the gas fired boilers (NFB), which is

89.58 tce ~316.37 tce. In the EVI system, the energy conservation effect of the system using R152a is the most obvious. Compared with the traditional heating methods using coal-fired boilers (CFB) and EHB, the energy saving is improved by 21.17%–38.86% and 64.05%–70.75%. Compared with the BASE system, the energy-saving of the EVI system using R152a, R410A, and CO_2 are increased by 10.15%–11.62%, 14.35%–15.07%, and 13.36%–21.07%, respectively. It can be found that the EVI system using CO_2 has the most obvious energy-saving effect compared with the BASE system, and the lower the ambient temperature is, the more obvious the energy-saving effect is.

Pollutant emissions including the gaseous and solid particle emissions are displayed in Figure 13. With the ambient temperature decreases, the emissions of the six pollutants continue to increase. Among all of the heating solutions, NFB always exhibits good emission characteristics. Compared with CFB and EHB, the EVI system has obvious advantages in the emission of six pollutants. Taking Harbin as an example, in Figures 13A, B, the highest emissions of CO_2 and CO using EHB are 2087.92 t and 1,675.36 kg, respectively, while the corresponding values of EVI system using R152a are 736.44 t and 590.92 kg, respectively, which are 62.73% and 64.72% lower than those of EHB. For SO_2 emissions, except for NFB, the EVI system using R152a has the least emissions. Compared with the other seven solutions, the emission reduction is increased by 3.73%–64.73% (Figure 13C). From Figure 13D, it can be seen that the EVI system using R152a has the smallest emissions, which is 3.72%–66.04% lower than the other eight heating schemes. For the emission of solid particles ($PM_{2.5}$, PM_{10}), Figures 13E, F show that the highest emissions of CFB are 1,180.41 kg and 2062.86 kg, which are 7.85 times and 8.03 times lower than those of the EVI system using R152a. Combined with Figure 10, the HSPF of the EVI system is generally higher than that of the BASE system, resulting in the highest power consumption under the same heat transfer. Therefore, the EVI system shows good emission characteristics over those of the BASE system.

5 Conclusion

In order to solve the heating problem in low-temperature areas, an air source heat pump (ASHP) system with enhanced vapor injection (EVI) using different low global warming potential (GWP) refrigerants is studied and compared with baseline heat pump (BASE) system and traditional heating solutions. The energy and environmental performance model of the ASHP used in five typical cities in the world are developed and optimized to evaluate the overall performance. Therefore, the conclusions are as follows:

(1) There is a maximum coefficient of performance (COP) when the working fluid CO_2 is used for EVI system at the optimum discharge pressure (p_h) and intermediate pressure (p_m). The maximum COP is 2.51, and the corresponding optimum p_h and p_m are 10.57 MPa and 3.83 MPa, respectively.
(2) The COP of R152a is the highest among all of the selected low GWP working fluids, which is 3.91 at the ambient temperature of 15°C. It also has good performance in low-temperature environment.
(3) The LCCP of the EVI system using CO_2, R410A, and R152a decreased by 15.34%–26.66%, 13.97%–17.01%, and 11.09%–13.10%, respectively, compared with the BASE system using the same working fluid. The lower the ambient temperature, the higher the emission reduction rate.
(4) SO_2 and NO_X of the EVI system using R152a are reduced by 3.73%–64.73% and 3.72%–66.04%, respectively, in contrast to the other seven heating schemes. For the emission of solid particles ($PM_{2.5}$, PM_{10}), the emissions of the EVI system using R152a are 7.85 times and 8.03 times lower than those of CFB in Harbin.

The work of this study will provide data reference for future simulation and experimental research in this field. In particular, the working fluid selection can help the manufacture and users to choose the proper working fluid, when the enhanced vapor injection technology is used for air source heat pump.

Data availability statement

The raw data supporting the conclusion of this article will be made available by the authors, without undue reservation.

Author contributions

LZ: Conceptualization, Data curation, Formal Analysis, Investigation, Writing–original draft, Writing–review and editing. WJ: Conceptualization, Data curation, Formal Analysis, Investigation, Writing–original draft, Writing–review and editing. QW: Conceptualization, Data curation, Formal Analysis, Investigation, Writing–original draft, Writing–review and editing. JZ: Writing–original draft, Writing–review and editing. PY: Writing–original draft, Writing–review and editing.

Funding

The author(s) declare that no financial support was received for the research, authorship, and/or publication of this article.

Conflict of interest

Authors LZ and WJ were employed by Zhejiang King Co., Ltd.

The remaining authors declare that the research was conducted in the absence of any commercial or financial relationships that could be construed as a potential conflict of interest.

Publisher's note

References

ANSI/ASHRAE (2013). *Climatic data for building design standards: ANSI/ASHRAE standard 169-2013*.

Chung, H., Baek, C., Kang, H., Kim, D., and Kim, Y. (2018). Performance evaluation of a gas injection CO_2 heat pump according to operating parameters in extreme heating and cooling conditions. *Energy* 154, 337–345. doi:10.1016/j.energy.2018.04.132

Dai, B., Hao, Y., Liu, S., Wang, D., Zhao, R., Wang, X., et al. (2022). Hybrid CO_2 air source heat pump system integrating with vapor injection and mechanical subcooling technology for space heating of global application: life cycle techno-energy-enviro-economics assessment. *Energy Convers. Manag.* 271, 116324. doi:10.1016/j.enconman.2022.116324

Dai, B., Liu, S., Li, H., Sun, Z., Song, M., Yang, Q., et al. (2018). Energetic performance of transcritical CO_2 refrigeration cycles with mechanical subcooling using zeotropic mixture as refrigerant. *Energy* 150, 205–221. doi:10.1016/j.energy.2018.02.111

Dai, B., Zhao, P., Liu, S., Su, M., Zhong, D., Qian, J., et al. (2020). Assessment of heat pump with carbon dioxide/low-global warming potential working fluid mixture for drying process: energy and emissions saving potential. *Energy Convers. Manag.* 222, 113225. doi:10.1016/j.enconman.2020.113225

de Carvalho, S. M. R., Massuchetto, L. H. P., do Nascimento, R. B. C., de Araújo, H. V., and d'Angelo, J. V. H. (2019). Optimization of a vapor injection refrigeration cycle using hydrocarbon mixed refrigerants. *Int. J. Refrig.* 98, 109–119. doi:10.1016/j.ijrefrig.2018.10.008

Farghali, M., Osman, A. I., Mohamed, I. M. A., Chen, Z., Chen, L., Ihara, I., et al. (2023). Strategies to save energy in the context of the energy crisis: a review. *Environ. Chem. Lett.* 21, 2003–2039. doi:10.1007/s10311-023-01591-5

Ghoubali, R., Byrne, P., Miriel, J., and Bazantay, F. (2014). Simulation study of a heat pump for simultaneous heating and cooling coupled to buildings. *Energy Build.* 72, 141–149. doi:10.1016/j.enbuild.2013.12.047

Gullo, P., Elmegaard, B., and Cortella, G. (2016). Energy and environmental performance assessment of R744 booster supermarket refrigeration systems operating in warm climates. *Int. J. Refrig.* 64, 61–79. doi:10.1016/j.ijrefrig.2015.12.016

Guo, Y., Guo, J., Yang, W., Zhao, P., Zhou, Y., Deng, R., et al. (2023). Experimental investigation on the heating performance of a R410A vapor-injection heat pump of an electric bus in cold regions. *Appl. Therm. Eng.* 222, 119938. doi:10.1016/j.applthermaleng.2022.119938

He, Y., Cheng, J., Chang, M., and Zhang, C. (2021). Modified transcritical CO_2 heat pump system with new water flow configuration for residential space heating. *Energy Convers. Manag.* 230, 113791. doi:10.1016/j.enconman.2020.113791

Heo, J., Jeong, M. W., and Kim, Y. (2010). Effects of flash tank vapor injection on the heating performance of an inverter-driven heat pump for cold regions. *Int. J. Refrig.* 33 (4), 848–855. doi:10.1016/j.ijrefrig.2009.12.021

IEA (2023). Outlooks for gas markets and investment. Available at: https://www.iea.org/reports/outlooks-for-gas-markets-and-investment (Accessed September 13, 2023).

Lee, H., Troch, S., Hwang, Y., and Radermacher, R. (2016). LCCP evaluation on various vapor compression cycle options and low GWP refrigerants. *Int. J. Refrig.* 70, 128–137. doi:10.1016/j.ijrefrig.2016.07.003

Li, K., Ma, J., Zhang, B., Su, L., Liu, N., Zhang, H., et al. (2023). Experimental study on low temperature heating performance of different vapor injection heat pump systems equipped with a flash tank and economizers for electric vehicle. *Appl. Therm. Eng.* 227, 120428. doi:10.1016/j.applthermaleng.2023.120428

Liu, Z., Ma, L., Qian, Z., and He, Y. (2023). Experimental study on performance of the trans-critical CO_2 heat pump with flash tank vapor injection at variable revolution ratio conditions. *J. Clean. Prod.* 412, 137405. doi:10.1016/j.jclepro.2023.137405

Llopis, R., Nebot-Andrés, L., Cabello, R., Sánchez, D., and Catalán-Gil, J. (2016). Experimental evaluation of a CO_2 transcritical refrigeration plant with dedicated mechanical subcooling. *Int. J. Refrig.* 69, 361–368. doi:10.1016/j.ijrefrig.2016.06.009

Lorentzen, G. (1994). Revival of carbon dioxide as a refrigerant. *Int. J. Refrig.* 17 (5), 292–301. doi:10.1016/0140-7007(94)90059-0

Maeng, H., Kim, J., Kwon, S., and Kim, Y. (2023). Energy and environmental performance of vapor injection heat pumps using R134a, R152a, and R1234yf under various injection conditions. *Energy* 280, 128265. doi:10.1016/j.energy.2023.128265

Mateu-Royo, C., Arpagaus, C., Mota-Babiloni, A., Navarro-Esbrí, J., and Bertsch, S. S. (2021). Advanced high temperature heat pump configurations using low GWP refrigerants for industrial waste heat recovery: a comprehensive study. *Energy Convers. Manag.* 229, 113752. doi:10.1016/j.enconman.2020.113752

Peng, X., Wang, D., Wang, G., Yang, Y., and Xiang, S. (2020). Numerical investigation on the heating performance of a transcritical CO_2 vapor-injection heat pump system. *Appl. Therm. Eng.* 166, 114656. doi:10.1016/j.applthermaleng.2019.114656

Qiao, H., Aute, V., and Radermacher, R. (2015). Transient modeling of a flash tank vapor injection heat pump system - Part I: model development. *Int. J. Refrig.* 49, 169–182. doi:10.1016/j.ijrefrig.2014.06.019

Sun, J., Guo, J., He, L., Hou, S., and Yu, Z. (2023). Comparative research on vapor injection heat pump with a novel flash tank. *Heliyon* 9 (6), e16485. doi:10.1016/j.heliyon.2023.e16485

Wang, W., and Li, Y. (2019). Intermediate pressure optimization for two-stage air-source heat pump with flash tank cycle vapor injection via extremum seeking. *Appl. Energy* 238, 612–626. doi:10.1016/j.apenergy.2019.01.083

Wang, Z., Wang, F., Ma, Z., Lin, W., and Ren, H. (2019). Investigation on the feasibility and performance of transcritical CO_2 heat pump integrated with thermal energy storage for space heating. *Renew. Energy* 134, 496–508. doi:10.1016/j.renene.2018.11.035

Wu, D., Hu, B., and Wang, R. (2021). Vapor compression heat pumps with pure Low-GWP refrigerants. *Renew. Sustain. Energy Rev.* 138, 110571. doi:10.1016/j.rser.2020.110571

Xu, X., Hwang, Y., and Radermacher, R. (2011). Refrigerant injection for heat pumping/air conditioning systems: literature review and challenges discussions. *Int. J. Refrig.* 34 (2), 402–415. doi:10.1016/j.ijrefrig.2010.09.015

Xu, X., Hwang, Y., and Radermacher, R. (2013). Performance comparison of R410A and R32 in vapor injection cycles. *Int. J. Refrig.* 36 (3), 892–903. doi:10.1016/j.ijrefrig.2012.12.010

Yang, T., Zou, H., Tang, M., Tian, C., and Yan, Y. (2022). Experimental performance of a vapor-injection CO_2 heat pump system for electric vehicles in −30 °C to 50 °C range. *Appl. Therm. Eng.* 217, 119149. doi:10.1016/j.applthermaleng.2022.119149

Yang, T., Zou, H., Tang, M., Tian, C., and Yan, Y. (2023). Comprehensive study on EEVs regulation characteristics of vapor-injection CO_2 heat pump for electric vehicles. *Int. J. Refrig.* 149, 11–22. doi:10.1016/j.ijrefrig.2022.12.015

Zhang, D., Li, J., Nan, J., and Wang, L. (2016). Thermal performance prediction and analysis on the economized vapor injection air-source heat pump in cold climate region of China. *Sustain. Energy Technol. Assessments* 18, 127–133. doi:10.1016/j.seta.2016.10.008

Zhao, Y., and Yu, J. (2023). Thermodynamic analysis of a modified vapor-injection heat pump cycle using an ejector. *Int. J. Refrig.* 145, 137–147. doi:10.1016/j.ijrefrig.2022.09.011

Nomenclature

A	area (m^2)
h	specific enthalpy (kJ/kg)
M	molecular weight
m	weight [kg(g)]
p	pressure (MPa)
p_h	discharge pressure (MPa)
Q	heating capacity (kW)
q	heat flux (W/m^2)
W	power consumption (kW)
Symbols	
0,1,2,3,4,5,6,7,8,9,1′,2′,3′,4′	state point
BASE	baseline
b	boiling point
Comp	compressor
c	critical
desi	design
emis	emission
g	global
H	heating
h	high
in	inlet
l	low
m	middle
out	outlet
w	water
Greek symbols	
μ_{emis}	emission conversion factor (kg (g)/kW h)
ρ	density (kg/m^3)
Acronyms	
ASHP	air source heat pump
BASE	basic heat pump system
EVI	heat pump system with enhanced vapor injection
HSPF	heating seasonal performance factor
CFB	coal fired boiler
CO_2	carbon dioxide
COP	coefficient of performance
EHB	electric direct heating boiler
GWP	global warming potential
HCFCs	hydrochlorofluorocarbons
HFCs	hydrofluorocarbons
LCCP	life cycle climate performance
NFB	gas fired boiler
ODP	ozone depression potential